Chapter 3

Influence of a transverse magnetic field on wakefield oscillations around a charged dust grain in complex plasma

In this chapter, the wakefield phenomena around a charged dust grain in a streaming complex plasma in the presence of an external magnetic field have been studied. Previous investigations have predominantly focused on the influence of a magnetic field aligned with the ion flow direction, leading to significant wakefield suppression. However, the influence of a transverse magnetic field, perpendicular to the ion flow direction, on the wakefield remains less explored. In this work, we present a comprehensive study of the wakefield characteristics when exposed to a transverse magnetic field relative to the ion flow direction with the help of Linear Response Theory. The effect of various factors, including the magnetic field strength, the ion flow velocity, and the ion-neutral collision frequency, on the wake potential profile has been extensively discussed.

3.1 Introduction:

The electric fields present in the RF sheaths or positive columns of DC discharge dusty plasma chambers play an important role in driving and controlling the behavior of ions within the plasma environment. These electric fields often lead to the flow of ions from the bulk plasma toward the boundaries of the chamber. These flowing ions affect the screening around the dust grains and modify the Debye sphere around the dust particles, introducing anisotropy in the interaction between two dust particles. Because of this, the potential around a dust grain deviates from the isotropic Yukawa potential. Basically, the ions in the system can exhibit two roles. First, these ions effectively shield the dust grains and give rise to a screened Coulomb potential, also known as the Yukawa potential. Second, the drifting ions (from bulk) are responsible for an overshielding mechanism due to the polarization of the background medium by the negatively charged dust grains. These ions distort the symmetric Debye cloud and induce a focusing effect.

The wake potential is the result of the resonant interaction between a test dust particle and dusty plasma collective modes [103]. The existence of the wake potential has been confirmed by several experimental and simulation studies in complex plasma systems [104; 162; 163; 105; 114]. Researchers have observed the formation of dust structures, such as vertical string-like configurations, which are attributed to the presence of attractive wake potential [112; 113]. Various groups have studied its influence on the behavior of strongly coupled plasma systems. Understanding the wake potential and its impact on the dynamics of complex plasma is important for investigating phenomena such as dust crystallization, self-organization, and collective behavior in the system. Overall, the drifting ions and the resulting wake potential play a significant role in shaping the behavior and structure of complex plasma systems, and their study contributes to our understanding of plasma physics and related phenomena.

In a pioneering work by Nambu *et al.*, it was demonstrated that when low-frequency waves interact with flowing ions and dust particles suspended in the electrostatic sheath of a plasma chamber, collective effects emerge, leading to the formation of an oscillatory wake potential along the direction of ion flow [103].

Remarkably, the strength of this potential is further amplified when an external magnetic field is introduced. The findings are applicable under specific conditions, namely, for supersonic ion flow with a Mach number (M) greater than 1 and when the value of $\frac{1}{fM^2}$ is less than 1, where $f = \frac{\omega_{pi}^2}{\omega_{ci}^2}$ represents the ratio of the square of the ion plasma frequency (ω_{pi}) to the square of the ion cyclotron frequency (ω_{ci}). Additionally, it is important to note that the magnetic field strength considered in their analysis was relatively weak. With the help of MD simulation, Ludwig *et al.* explored the effects of ion flow on dust grain ordering and related phase transitions in complex plasmas [107]. Their research revealed that intense ion flows could play a pivotal role in the creation of vertical chains formed by dust grains. Nowadays, several laboratories and fusion devices offer the capability to access high magnetic fields experimentally. However, achieving magnetization for massive dust grains (with a mass of approximately 10^{-15} kg) poses a challenge since the criteria required for dust grain magnetization are difficult to meet. Experiments like the Magnetized Dusty Plasma Experiment (MDPX) are currently underway, and they highlight the necessity of simultaneously fulfilling the requirements of a large magnetic field and a small particle size to successfully magnetize grains. Smaller dust grains, being less affected by the force of gravity, can be readily levitated by the electric field present in the bulk plasma. This favorable environment of a strong magnetic field opens up numerous new possibilities for investigating organized structures in complex plasmas. Schwabe *et al.* examined the influence of ion magnetization in the presence of a powerful magnetic field [164]. Through experimental observations, they established a direct correlation between the magnetization of ions, the strength of filamentation, and the induced rotation of a plasma crystal within this strong magnetic field environment. In their study, Nambu and colleagues investigated the effects of a high magnetic field on the three-dimensional wake potential, considering the $E \times B$ drift in a supersonic ion flow [165]. They explored how the interplay between the electric and magnetic fields influences the wake potential in this complex plasma environment [165]. In the presence of a magnetic field applied perpendicular to the flow of ions, Bezbaruah *et al.*, obtained a simple expression for wake potential in a 2-D magnetized complex plasma using Linear Response Theory [162]. They have studied the effect of the wake potential on governing the structural proper-

ties of strongly coupled dusty plasma in the presence of a moderate to relatively strong field strength.

In most of the works mentioned above, the collisions between different plasma species were not taken into account. Bezbaruah *et al.* have studied the effect of ion-neutral collision on interaction potential in the strong collisional limit [166]. It was observed that the usual mechanism of ion focusing surrounding the grain is inhibited due to collision. As a result, the attractive wake potential structure is destroyed in the strong collisional limit. The collisions between different plasma species play a pivotal role in determining self-organization, phase transition, and transport properties. It becomes essential to consider the collision of the plasma species (ions) with the neutrals when the ion-neutral mean free path (λ_{mfp}) is small enough in comparison to the wavelength of collective modes and other characteristic lengths in the system. As a consequence, the dielectric properties of the plasma medium are altered, leading to modifications in the interaction potential experienced by a test particle. These changes in the interaction potential have important implications for understanding the behavior and interactions of particles in plasmas, highlighting the complex interplay between various physical effects in such systems.

The main objective of the present work is to understand the behavior of wake potential in the presence of moderate ion-neutral collisions. We have derived mathematical expressions to describe the interaction between dust grains in the presence of ion flow and a magnetic field. This can help us understand how collisions, ion flow, and magnetic fields affect processes such as dust crystallization and phase transitions, as well as the transport of mass and energy in systems with ion flow and magnetic fields.

3.2 Theoretical Model:

In the present analysis, we have considered negatively charged dust grains embedded in a plasma consisting of electrons, ions, and neutrals. The electrons are considered to obey the Boltzmann distribution in the present theory. The devia-

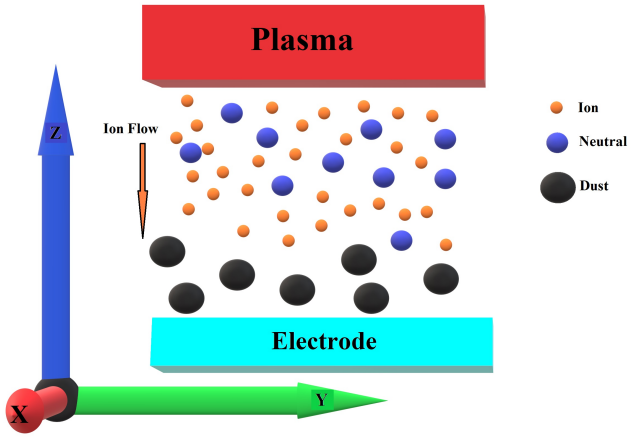

Figure 3.1: A 3D dusty plasma with streaming ions and an external magnetic field applied along the X-direction.

tion from Boltzmann equilibrium is observed in the presence of a strong magnetic field in the bulk plasma region. Nonetheless, the current model primarily addresses dust particles suspended in the proximity of the sheath region, where electrons continue to conform to the Boltzmann distribution even in the presence of a moderate magnetic field, as outlined below-

$$n_e = n_0 \exp\left(\frac{e\phi}{k_B T_e}\right)$$

.

The electron temperature being sufficiently high ($\approx 10^4$ K), the species get thermalized and behave as classical gas in the ion time scale. In the present work, the plasma sheath region which encounters a strong flow of ions due to electrostatic sheath potential is the main regime of interest. The ions are streaming in the vertical Z-direction and obey the full equation of motion in the background of massive dust grains. In our analysis, we have used the fluid equations as an analytical tool to derive the expression for the dispersion relation. As described in Chapter 2, the ions can be described by the following equations:

$$\frac{\partial v_i}{\partial t} + (v_i.\nabla)\, v_i = \frac{e}{m_i} E + \frac{e}{m_i}\,(v_i \times B) - v_i \nu_{in} - \frac{\nabla P}{n_i m_i}$$

$$\frac{\partial n_i}{\partial t} + \nabla.\,(n_i v_i) = 0$$

$$\nabla^2\Phi = 4\pi[en_i - en_e]$$

The above 3 equations correspond to the momentum equation, continuity equation, and Poisson's equation, respectively. Here, m_s represents the mass of a species s, n_s stands for the number density of a species s, v_s indicates the velocity of species s, Q_s denotes the charge carried by species s, E signifies the electric field, B represents the magnetic field, and P stands for pressure. Additionally, n_s specifically refers to the density of the particular species s within the plasma, while $\mathbf{v}_s$ expresses the velocity vector of species s. Linear response formalism is a powerful tool for understanding how the system reacts to small disturbances, focusing on first-order perturbations around an equilibrium state. It involves expressing perturbed quantities like velocities and densities in terms of their equilibrium values and perturbations. Additionally, transforming space and time dependencies into wave vector and angular frequency terms facilitates the analysis of wave-like behaviors within the system, often achieved through Fourier transforms of the governing fluid equations.

$$\mathbf{v}_s = \mathbf{v}_{s0} + \mathbf{v}_{s1}$$

$$n_s = n_{s0} + n_{s1}$$

Here, $\mathbf{v}_s$ represents the total velocity of species 's', $\mathbf{v}_{s0}$ is the unperturbed (equilibrium) velocity, and $\mathbf{v}_{s1}$ is the velocity perturbation, n_s represents the total number density of species 's', n_{s0} is the unperturbed (equilibrium) density, and n_{s1} is the density perturbation. Utilizing the principles of fluid equations, we derive the dielectric response function denoted as $\epsilon(\omega, k)$.

$$\epsilon(\omega,k) = 1 + \frac{1}{k^2\lambda_{De}^2} + \frac{\omega_{pi}^2(-k\cdot u_{i0} + i\nu_{in})}{k\cdot u_{i0}\left[(-k\cdot u_{io} + i\nu_{in})^2 - \omega_{ci}^2\right] + \left((-k\cdot u_{io} + i\nu_{in})k^2 v_{Ti}^2\right)} \quad (3.1)$$

Normalizing equations in physics is a valuable technique for simplifying, comparing, and gaining deeper insights into physical phenomena. Here, the dielectric response function is normalized with respect to both length and frequency scales, using the Debye length (λ_{De}) and plasma frequency (ω_{pi}) as reference values. After normalizing, we obtain the steady-state dispersion relation with the following

expression

$$\epsilon(0,k) = 1 + \frac{1}{k^2} + \frac{\beta}{k.M(\beta^2 - f_i^2) + \beta k^2} \tag{3.2}$$

The dielectric response function takes account of various model features considered in the system. In the above equation, the parameter β is defined as $\beta = -k.M + i\nu_{in}$, where M represents the normalized ion flow velocity (Mach number), and ν'_{in} represents the normalized ion-neutral collision frequency. The normalized ion flow velocity is given by $M_i = \frac{u_i}{\omega_{pi}\lambda_{De}}$, where u_i represents the ion drift velocity, ω_{pi} is the ion plasma frequency, and λ_{De} is the Debye length. The normalized ion cyclotron frequency is given by $f_i = \frac{\omega_{ci}}{\omega_{pi}}$, where ω_{ci} represents the ion cyclotron frequency. Additionally, the wave vector of the electrostatic ion cyclotron mode is expressed as $k^2 = k_\parallel^2 + k_\perp^2$, where $k_\parallel$ and $k_\perp$ represent the parallel and perpendicular components of the wave vector with respect to the ion flow, respectively. The previously mentioned dielectric response function in Equation (3.2) is derived by employing the approximation $k_\parallel^2 > k_\perp^2$. The term $\nu_{in} = \sigma_{in} n_n V_{Ti}$ represents the collision frequency between ions and neutrals, where σ_{in} stands for the collision cross-section, n_n denotes the density of neutrals, and v_{Ti} represents the thermal speed of ions.

3.3 Interaction potential:

The electrostatic potential surrounding a test dust particle can be obtained by using the following expression:

$$\Phi = \frac{Q_d}{(2\pi)^2 \lambda_{De}\epsilon_0} \int dk_\perp \exp(ik_\perp z) \int \frac{dk_\parallel \exp(ik_\parallel y)}{k^2 \epsilon(0,k)} \tag{3.3}$$

The equation for the inverse of the steady-state response function given by equation (3.2) can be expressed as

$$\frac{1}{\epsilon(0,k)} = \frac{k^2}{k^2+1} - \frac{k^2}{k^2+1} \frac{\beta}{(k^2+1)[M(\beta^2 - f_i^2) + \beta k] + \beta} \tag{3.4}$$

The above expression is substituted in equation (3.6) to get the following result:

$$\phi = \frac{Q_d}{(2\pi)^2 \lambda_{De}\epsilon_0} \int dk_\perp \exp(ik_\perp z) \int \frac{dk_\parallel \exp(ik_\parallel y)}{k^2} (\beta_1 - \beta_2) \tag{3.5}$$

Here,

$$\beta_1 = \frac{k^2}{k^2+1}$$

,

$$\beta_2 = \frac{k^2}{k^2+1}\frac{\beta}{(k^2+1)[M(\beta^2-f_i^2)+\beta k]+\beta}$$

After solving the integral for the first part inside the bracket (β_1), we get the normal Debye – Hückel (Yukawa potential) Potential in the form-

$$\phi_Y = \frac{Q_d}{4\pi\epsilon_0 r} exp\left(-\frac{r}{\lambda_D}\right) \tag{3.6}$$

Here, λ_D is the Debye screening length ($\lambda_D = \sqrt{\frac{k_B T_i}{4\pi n_i e^2}}$) and Q_d is the dust charge. Now putting the second part inside the bracket (β_2), we get -

$$\phi_w = \frac{Q_d}{(2\pi)^2\lambda_{De}\epsilon_0}\int dk_\perp \exp(ik_\perp z)\int \frac{dk_\parallel \exp(ik_\parallel y)}{k^2}\left(\frac{k^2}{k^2+1}\frac{\beta}{(k^2+1)[M(\beta^2-f_i^2)+\beta k]+\beta}\right) \tag{3.7}$$

Now, we can proceed to solve the equation numerically by employing specific values for the model parameters. These parameters include particle properties, plasma conditions, and external field strengths, which are carefully chosen to accurately represent the system under investigation. By selecting appropriate values for these parameters, we aim to capture the relevant physical phenomena and dynamics of the complex plasma. In the results and discussions section, we present the outcomes of the numerical results. These results provide a deeper understanding of the system's dynamics and contribute to advancing our knowledge in the field. In the table below, some input parameters are shown that we have used in our simulation, all of which hold significance for experiments centered around complex plasmas.

3.4 Results and discussions:

3.4.1 The variation of wake potential with Mach numbers:

1. Subsonic regime:

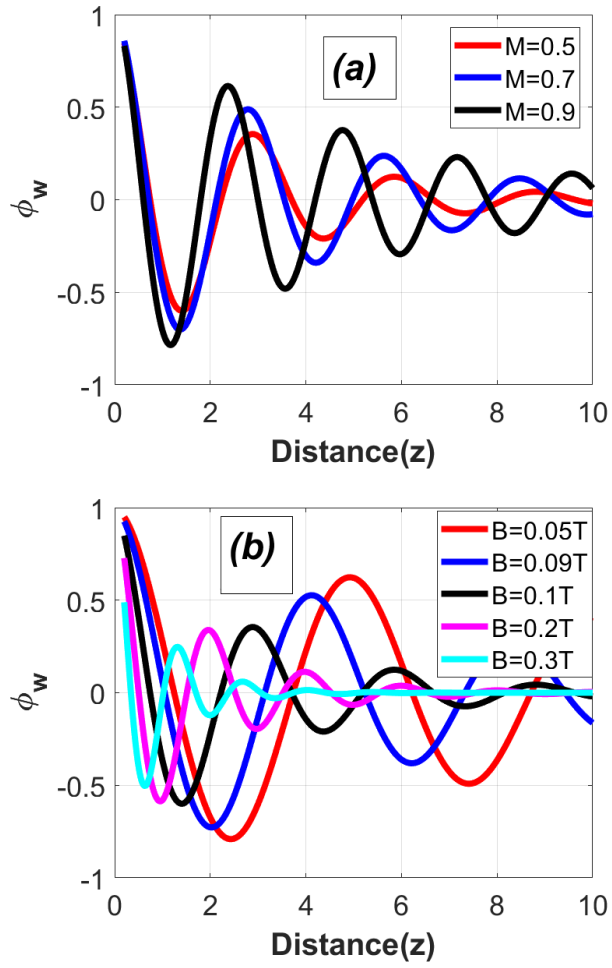

Figure 3.2: (a) The variation in the strength of wake potential along the streaming axis for a set of Mach numbers in the subsonic regime at $B = 0.1$ T and $\nu_{in} = 0.1$ (b) Wake potential along the streaming axis for different magnetic field strengths in the subsonic regime for $M = 0.5$.

Parameter	Typical Value
Electron density (n_e)	$\approx 10^{14}\,\mathrm{m}^{-3}$
Ion density (n_i)	$\approx 10^{15}\,\mathrm{m}^{-3}$
Neutral density (n_d)	$\approx 10^{15}\,\mathrm{m}^{-3}$
Dust density (n_d)	$\approx 10^{11}\,\mathrm{m}^{-3}$
Electron temperature (T_e)	$\approx 10^{4}\,\mathrm{K}$
Ion temperature (T_i)	$\approx 10^{3}\,\mathrm{K}$
Dust temperature (T_d)	$\approx 10^{2}$-$10^{3}\,\mathrm{K}$
Dust Charge (Q_d)	$\approx 10^{3}\,e$
Mean particle distance (r_{av})	$\approx 10^{-4}\,\mathrm{m}$
Dust Debye length (λ_d)	$\approx 10^{-4}\,\mathrm{m}$
Ion plasma frequency (ω_{pi})	$\approx 10^{6}\,\mathrm{s}^{-1}$

Table 3.1: Typical dusty plasma parameters [8; 9; 10].

The variation of wake potential along the streaming axis for different values of Mach numbers ($M = 0.5$ to $M = 0.9$) in the subsonic regime is shown in Fig. 3.2(a). It is observed that the periodicity of consecutive oscillations in the wake is amplified with higher Mach numbers, leading to distinct and sustained long-range oscillatory structures in this regime. Additionally, the amplitude of the wake potential indicates an increasing trend as the Mach number rises within this subsonic regime. A significant indication of these results is the stronger ion-focusing effect associated with higher Mach numbers, particularly in the case of moderate ion flow velocities. In Fig. 3.2(b), the influence of the transverse magnetic field (with field strengths $B = 0.05\,\mathrm{T}$, $B = 0.09\,\mathrm{T}$, $B = 0.1\,\mathrm{T}$, $B = 0.2\,\mathrm{T}$, and $B = 0.3\,\mathrm{T}$) on the wake potential is investigated at normalized flow velocity $M = 0.5$. The damping of the wake amplitude is observed with the rise in the magnetic field. Previously reported studies on wakefields have also shown that when an external magnetic field is applied along the flow direction (parallel to the ion flow), the wake oscillations are significantly suppressed [106; 167]. With the increase in magnetic field strength in a complex plasma system, charged particles, like ions, experience a stronger Lorentz force, which confines and

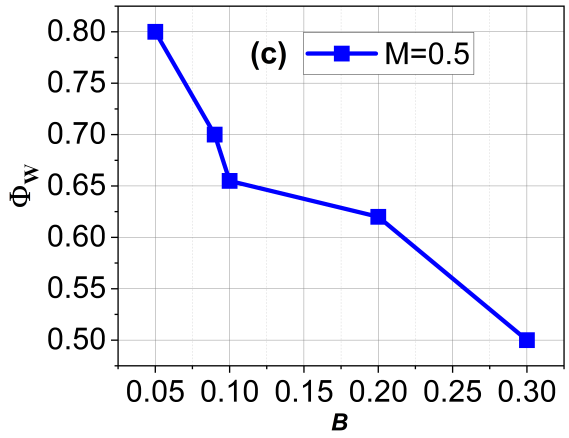

Figure 3.2: (c) Variation of the maximum of the peak amplitudes of the wake potential as a function of B.

guides them along the magnetic field lines, disrupting ion focusing and restricting their transverse movement. The relationship between the wake peak height and B is depicted in Fig. 3.2(c). As the magnetic field increases, there is a noticeable reduction in the height of the first peak of the wake amplitude in this subsonic regime.

2. Supersonic regime:

In Fig. 3.3(a), the variation of wake potential along the streaming axis for different values of Mach numbers ($M = 0.5$ to $M = 0.9$) in the supersonic regime is presented. Observations reveal that higher Mach numbers in this regime lead to a reduction in the periodicity or spacing between consecutive wake oscillations, accompanied by a decreasing trend in the amplitude of the wake potential. Notably, these results indicate a weaker ion-focusing effect associated with higher Mach numbers, especially for higher ion flow velocities. The observed behavior can be attributed to the interplay between two crucial factors: the increase in the number of influx ions into the wake region and the larger kinetic energy of the streaming ions with increasing ion flow speed in the supersonic regime. In the subsonic regime, as the ion flow speed rises, a greater number of ions are drawn into the wake region, leading to an enhanced ion focusing effect and resulting in

the enhanced periodicity of wake oscillations, as illustrated in Fig. 3.2(a). On the other hand, in the supersonic regime, the higher kinetic energy of the ions can cause particles in the wake region to have an increased escape ability. The ions may have enough kinetic energy to overcome the attractive forces and escape the wake region. As a result, the concentration of ions in the wake might decrease, resulting in a reduction in the periodicity of wake oscillations, accompanied by a decreasing trend in the amplitude of the wake potential. In Fig. 3.3(b), the influence of the transverse magnetic field (with field strengths $B = 0.05\,\mathrm{T}$, $B = 0.09\,\mathrm{T}$, $B = 0.1\,\mathrm{T}$, $B = 0.2\,\mathrm{T}$, and $B = 0.3\,\mathrm{T}$) on the wake potential is investigated at normalized flow velocity $M = 1.5$. As in the subsonic case, the damping of the wake amplitude is observed with the rise in the magnetic field. The relationship between the wake peak height and B in the supersonic regime is depicted in Fig. 3.3(c). An observable decrease in the peak height of the wake amplitude within this range becomes evident with an increase in the strength of the magnetic field.

3.4.2 Effect of ion-neutral collisions on wake profile:

We now investigate the influence of ion-neutral collisions in complex plasma. In a complex plasma, ions can undergo frequent collisions with neutral particles in the plasma. These collisions can lead to energy loss for the ions and the trapping of ions within the potential well surrounding the negatively charged dust grains. This phenomenon is known as *ion trapping*. Once trapped, they can oscillate around the dust grain, being influenced by the combined effects of the electrostatic potential and the external magnetic field (if present). This trapping mechanism is a consequence of the balance between the attractive force of the potential well and the ion's thermal energy. In this discussion, we will explore and analyze both the weak and strong collisional limits.

(a) Weak and moderate collisional case

In Fig. 3.4(a), the variation of wake potential along the streaming axis for different values of collision frequencies is presented, representing a scenario characterized

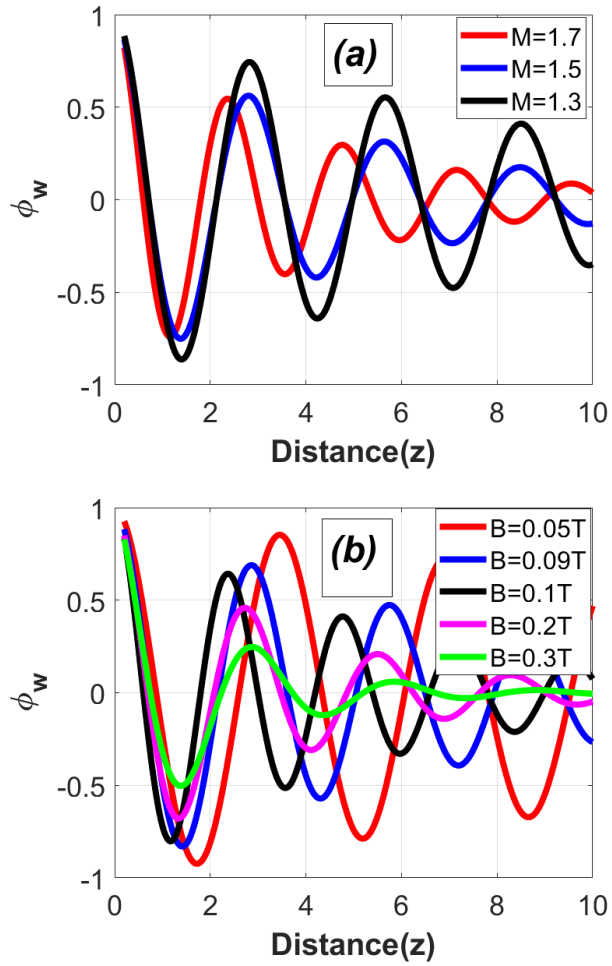

Figure 3.3: (a) The variation in the strength of wake potential along the streaming axis for a set of Mach numbers in the supersonic regime at $B = 0.1$ T and $\nu_{in} = 0.1$ (b) Wake potential along the streaming axis for different magnetic field strengths in the supersonic regime for $M = 0.5$.

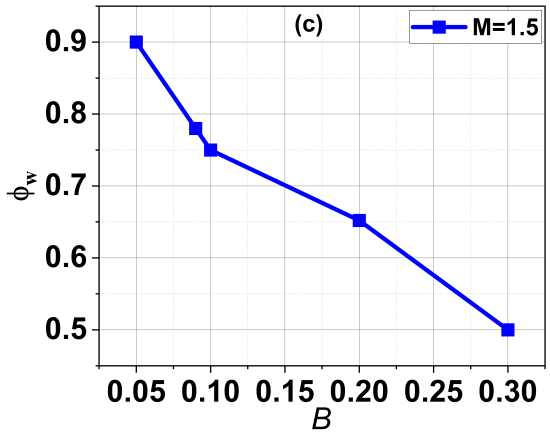

Figure 3.3: (c) Variation of the maximum of the peak amplitudes of the wake potential as a function of B.

by weak collisions. In this context, we do not observe any pronounced variation in the amplitude and profile of the wake potential. This indicates that the effects of weak collisions on the wake dynamics are relatively subtle and do not significantly alter the overall behavior of the wake potential as it propagates along the streaming axis. Fig. 3.4(b) demonstrates the way in which the maximum peak amplitudes of the wake potential evolve as the collision frequency varies within the weak collisional limit. In this context, there are no significant or noteworthy shifts in the peak amplitude of the wake potential.

(b) Strong collisional case

In Fig. 3.5(a), we investigate the behavior of the wake potential along the streaming axis by considering different values of collision frequencies, focusing on a scenario characterized by very strong collisions. In this context, we observe a significant reduction in the amplitude of the wake potential. As the collision frequency becomes very high (e.g., $\nu = 10$), the oscillatory structure of the wake potential completely disappears, as it is visually evident in the figure. This indicates that the presence of strong collisions profoundly affects the wake dynamics, leading to

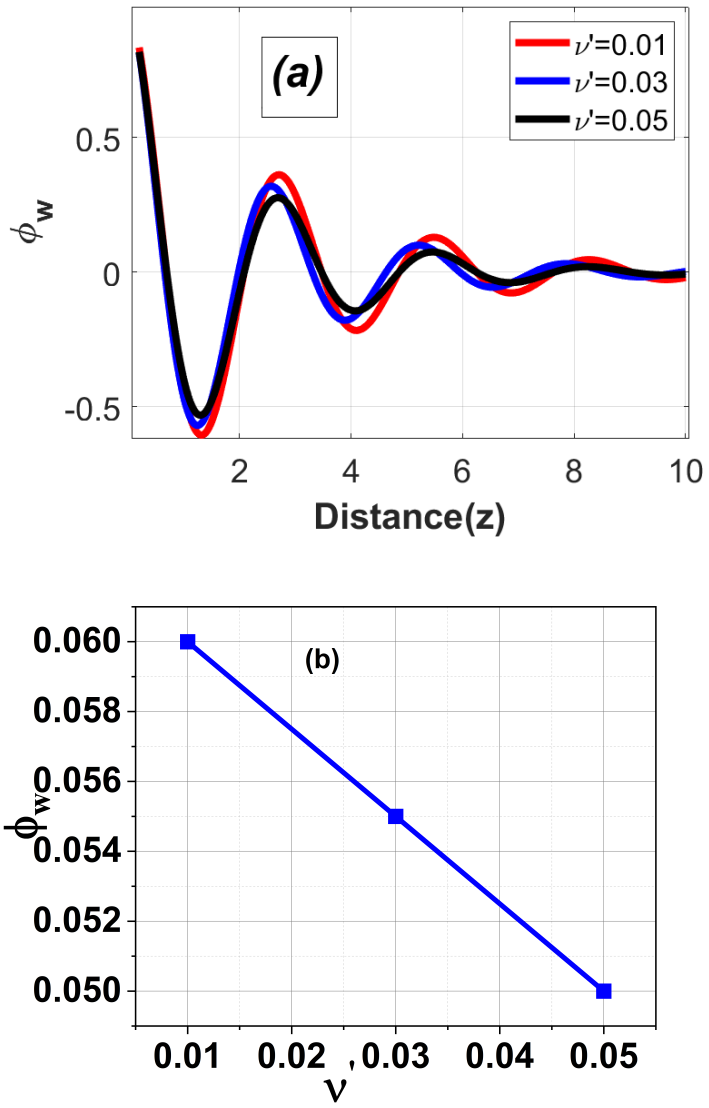

Figure 3.4: (a) The variation in the strength of wake potential for a set of ion-neutral collision frequency at $B = 0.1$ T and $M = 0.5$ (b) Variation of the maximum of the peak amplitudes of the wake potential as a function of collision frequency in weak collisional limit.

a notable damping of the wake potential's amplitude and the eventual suppression of its oscillatory features. Fig. 3.5(b) depicts the maximum peak amplitudes of the wake potential as the collision frequency changes under the conditions of strong collisions. In this situation, a noticeable reduction in the height of the peak amplitude of the wake potential can be observed within this specific range.

In the context of strong collisions, our findings closely align with those of Bezbaruah

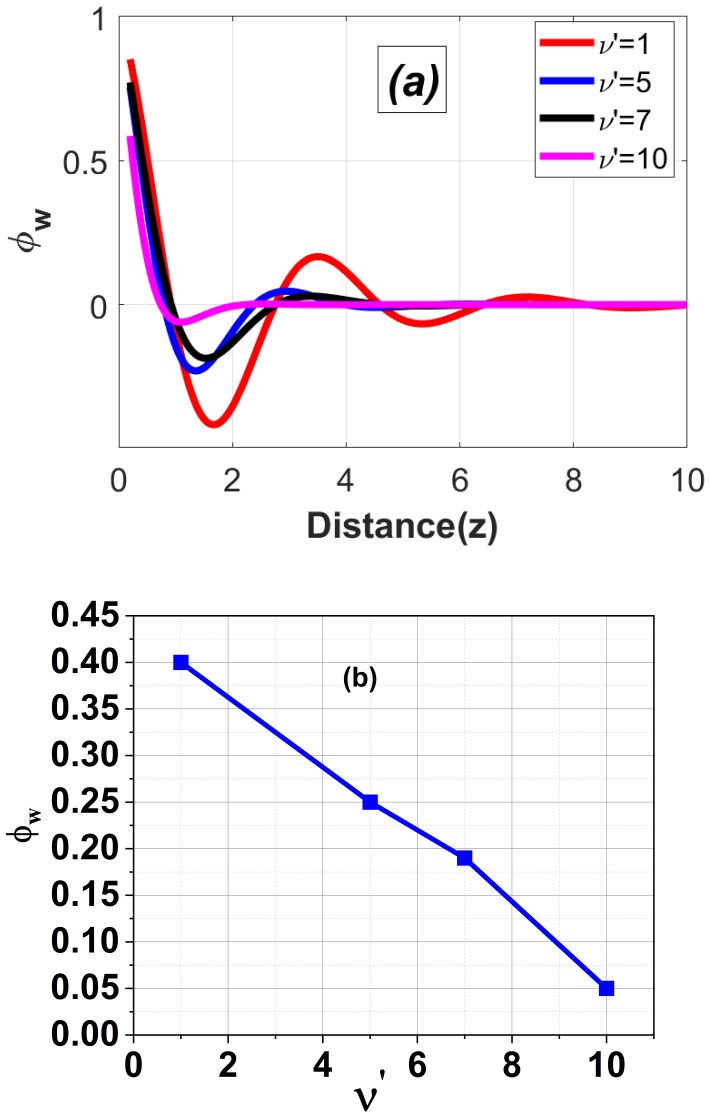

Figure 3.5: (a) The variation in the strength of wake potential for a set of ion-neural collision frequency at $B = 0.1$ T and $M = 0.5$ (b) Variation of the maximum of the peak amplitudes of the wake potential as a function of collision frequency.

et al., who also observed similar outcomes under strong collisional conditions [166]. Using Liner response theory they found that when ion-neutral collisions are very prominent, the attractive oscillatory potential is entirely eliminated. The disappearance of the wake potential can be attributed to the influence of the impact of these collisions, which disturbs the ion-focusing effect. These findings carry particular significance in the realm of experiments involving dusty plasmas, where the influence of ion-neutral collisions is substantial.

3.5 Comparison with experiments:

Puttscher *et al.*, reported on the vertical alignment of two dust particles levitated in the sheath region of an rf-discharge in the presence of an external magnetic field transverse to the sheath electric field due to the ion focusing effect.[7] The dependence of the attractive wake potential derived in the present work on Mach number (M), magnetic field (B) and collision frequency (ν_{in}) are in good agreement with the observations of Puttscher *et al.*, where they had demonstrated the alignment of two dust particles along the sheath electric field basically due to the attractive force arising due to ion focusing. On increasing the magnetic field, they observed a horizontal displacement between upper and lower particles, indicating a weakening of the attractive force. The mechanism can very well be explained based on the results of wake potential along the streaming axis for different magnetic field strengths in the subsonic and supersonic regime. The amplitude of wake potential is found to decrease when the magnetic field (B) is increased both in subsonic and supersonic regimes. The ion focusing gets disturbed when the trajectory of the ions is deflected due to Lorentz force. They also found that the pair of dust particles can be easily dissociated by using a smaller magnetic field when the gas pressure is relatively high. The collision of ions with gas particles results in the scattering of ions, thus reducing the ion focusing. Our results clearly indicate that the wake potential significantly gets damped when the collision frequency $\nu_{\mathbf{in}}$ is increased. In their experiment, Puttscher *et al.,* measured horizontal separations between upper and lower dust particles with varying magnetic fields in the milli Tesla range. The strength of the attractive ion focusing force was estimated by applying radiation pressure due to a focused laser beam. In Fig. 3.6, we have compared the force derived from combined Yukawa and wake potential with B vs Δx (horizontal displacement) plot of Puttscher *et al.*. The neutral pressure is fixed at 1 Pa that corresponds to $\nu'_{in} = 0.025$.

Although the parameters used in the experiment do not exactly match with those used in our theory, the overall trend of the horizontal displacements of pair of dust particles in the experiment by Puttscher *et al.* can be explained on the basis of wake potential derived in the present work for collisional case. The displacement is found to be maximum corresponding to magnetic field where the ion

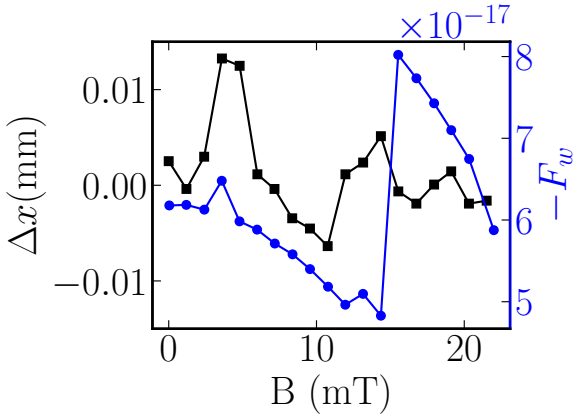

Figure 3.6: A comparison between the ion focusing force (F_w) and the horizontal displacements (Δx) between two vertically aligned dust particles (data taken from Puttscher *et al.*[7]) for a range of magnetic fields. The comparison in blue for theoretical data and in black for experimental data helps to visualize the agreement between predicted and observed behaviors under similar conditions.

focusing force is minimum and vice versa. For B = 6 to 11 mT, the attractive force decreases while the horizontal displacement increases. At $B = 14$ mT, the attractive force takes its highest (most negative) value, whereas the horizontal displacement is significantly reduced. The alignment of dust particles for a particular magnetic field is synchronized with the ion-focusing force derived from the present theory. However the observed displacement does not match well with the force due to ion focusing near B=10 mT.

One issue of concern may be the role of ion magnetization on the ion-focusing attractive force. The ion magnetization may be characterized by the parameter f_i defined as $\frac{\omega_{ci}}{\omega_{pi}}$. In the present theory, the mass of an ion is chosen to be equal to m_p, the mass of a proton, assuming H^+ plasma. For the parameter considered here, $\omega_{ci} \approx \omega_{pi}$ for $B \geq 0.2\,\mathrm{T}$. At this value of magnetic field ion Larmour radius is almost equal to $r_{Li} = 1.253\lambda_{De}$ and the Hall parameter $H_i = \frac{\omega_{ci}}{\nu_{in}} \geq 1$. In the results of Fig. 3.6, it is however found that the ion focusing force gets

affected even for a magnetic field lower than 0.2 T. The ion trajectories may be influenced by a magnetic field even if ions are not fully magnetized, thus affecting the focusing of ions behind dust particles.

3.6 Conclusions:

In this study, we have conducted a comprehensive investigation into the behavior of wake potentials in complex plasma environments, considering various regimes, magnetic field strengths, and ion-neutral collision scenarios. Our findings explore the intricate interplay of various factors influencing wake dynamics and offer valuable insights into the fundamental principles governing these phenomena.

In the subsonic regime, we observed that higher Mach numbers amplify the periodicity of wake oscillations, resulting in sustained long-range oscillatory structures. Furthermore, higher Mach numbers exhibited a stronger ion-focusing effect, particularly at moderate ion flow velocities. The application of a transverse magnetic field led to the damping of the wake amplitude, consistent with previous studies highlighting the suppression of wake oscillations under such conditions. Conversely, in the supersonic regime, we found that higher Mach numbers reduce the periodicity between wake oscillations and decrease the amplitude of the wake potential. This behavior indicates a weaker ion-focusing effect, particularly for higher ion flow velocities. These observations are attributed to the balance between an increased influx of ions and higher kinetic energy, resulting in decreased ion concentration within the wake region.

Our investigation into ion-neutral collisions in complex plasmas revealed intriguing results in both weak and strong collisional cases. In weak collision scenarios, we observed subtle effects on wake dynamics, with no significant alteration of the wake potential's behavior. In moderate collision cases, however, we observed a substantial reduction in wake potential amplitude, and at very high collision frequencies, the wake's oscillatory structure disappeared entirely. These findings align with previous research and emphasize the substantial influence of ion-neutral collisions on wake potential dynamics. The disappearance of the wake potential

under strong collisions has implications for dusty plasma experiments, where the impact of ion-neutral interactions is substantial. Thus, attractive wake potential manifests in a dusty plasma environment only in the presence of weak to moderate ion-neutral collisions. The study also revealed that interactions among dust grains can be tuned by controlling parameters like magnetic field and gas pressure. It is the tunable wake potential that can be utilized in complex plasma to explore magnetorheological behavior even in small magnetic field regimes, which is possible in weakly collisional dusty plasma. In Chapter 5, we have explored how an external magnetic field influences the rheological properties of complex plasma via tunable wake potential.

In developing the present model for wake potential, it is assumed that ion streaming is uniform in the sheath regime. This assumption is consistent with the parameter regime taken from a typical dusty plasma laboratory environment. It is known from the literature that velocity shear may drive instabilities like Kelvin-Helmholtz (KH) and Inhomogeneous Energy-Density Driven Instabilities (IEDD). The temperature anisotropy arising due to these instabilities may influence the behavior of the wake potential. However, the possibility of growth of KH instability is very low when the inhomogeneity scale length of the velocity $\left|\frac{u_{i0}}{\frac{\partial u_{i0}}{\partial z}}\right| > r_{Li}$, the ion Larmor radius. This instability has limited application unless the second derivative of the electric field driving the ion flow is sufficiently large. Moreover, the present theory is based on the assumption that $\vec{E} \times \vec{B}$ drift is negligible due to the condition $k_z \gg k_y$. In the parameter regime where the growth rate of shear flow-induced instabilities is less, the Yukawa potential will not be affected by inhomogeneous ion flow. IEDD type instabilities may, however, arise when the cross-field flow velocity is sufficiently large and localized in space so that the Doppler shifted frequency $(\omega - k_z v_E)$ may become negative (where $v_E = cE_0/B_0$). In such situations, inhomogeneity in ion flow may affect the nature of the wake potential to some extent.